



Copper Gelled Chitosan: a Promising Material for Packaging Applications

Marwa Wahba ^{1*} and Ghada Awad ²

¹ Department of chemistry of natural and microbial products, National Research Centre, Egypt

² Pharmaceutical and Drug Industries Research Division, National Research Centre, Egypt



CrossMark

In Loving Memory of Late Professor Doctor "Mohamed Refaat Hussein Mahran"

Abstract

Both copper (Cu) and chitosan (CSN) are known for their antimicrobial traits. Hence, copper gelled chitosan (Cu-G-CSN) films were prepared in order to be utilized in packaging applications. Initially, the CSN solution was frozen and then the gelling Cu solution was placed over it. The slow diffusion of Cu into the solid frozen CSN would slow the rate of the Cu induced CSN gelation. Slow gelation was formerly shown to create more mechanically stable gels that exhibit more homogeneity. The homogeneity of the newly formed Cu-G-CSN elevated its barrier traits against water diffusion and inhibited the films swelling. Actually, no swelling and no significant weight alterations (p value > 0.05) were observed in the Cu-G-CSN samples, which were gelled with 0.5–2% CuSO_4 , after their immersion in distilled water for 48h at 37°C . The Cu-G-CSN films also offered considerable mechanical stability where a 12.84 ± 0.55 MPa tensile strength and $31.86 \pm 3.05\%$ elongation percent were recorded for the films gelled with 0.5% CuSO_4 . The newly formed Cu-G-CSN films were also characterized via UV-visible spectroscopic analysis and scan electron microscopy. Moreover, the antimicrobial traits of the Cu-G-CSN films were proven. All the tested Cu-G-CSN films exhibited antimicrobial activities against both *Staphylococcus aureus* and *Candida albicans*. These antimicrobial activities increased gradually upon increasing the concentration of the CuSO_4 in the gelling solution from 0.2 to 2%. The 2% CuSO_4 gelled films induced inhibition zones of 40 and 40.5 mm in case of *S. aureus* and *C. albicans*, respectively.

Keywords: Chitosan; Copper sulfate; packaging; antimicrobial.

1. Introduction

Chitosan (CSN) is the de-acetylation product of chitin; the second widespread natural polysaccharide. Thus, CSN is readily gettable. CSN is also biodegradable, safe and biocompatible [1]. Accordingly, CSN has been involved in a wide assortment of applications, such as tissue engineering, drug targeting [2] and enzymes immobilization [3]. An assortment of CSN based covalent immobilizers were developed. These immobilizers adopted CSN either as their main constituting material [4,5] or as an activator for the main constituting biopolymers [6,7]. CSN was also involved in wound dressing fabrication [8] owing to its antimicrobial attributes [1, 9]. CSN antimicrobial attributes would also be beneficial in food packaging as microbial spoilage causes the loss of hefty amounts of foods every year [10]. Furthermore, CSN manifests superior film forming capacity, and this further encouraged its inspection as food packaging material [2, 9, 11].

Noteworthy, CSN is acknowledged for its chelation capacity. CSN amino and, to a lesser extent, hydroxyl entities contribute their electron lone pairs to form co-ordinate bonds and chelate metal ions [1]; such as copper. Cu-CSN interactions are robust to the extent that CSN beads were concocted after dripping CSN onto copper sulfate solution. These beads were inspected as vehicles for insulin controlled release and also as cattle micronutrient supplement after the incorporation of riboflavin [12, 13]. On another occasion, the gelling copper sulfate solution was supplemented with glutaraldehyde in order to attain covalently reactive copper gelled CSN (Cu-G-CSN) beads, which were utilized for β -galactosidase immobilization [14]. However, Cu-G-CSN was not investigated for packaging applications although Cu is well acknowledged for its antimicrobial attributes [15, 16]. Thus, Cu-G-CS films were concocted herein as a promising antimicrobial packaging material.

Packaging materials should exhibit fine mechanical attributes in order to keep their

* Corresponding author: drmarwawahba@yahoo.com

Receive Date: 22 December 2023, Revise Date: 09 January 2024, Accept Date: 28 January 2024

DOI: 10.21608/ejchem.2024.257256.9015

©2024 National Information and Documentation Center (NIDOC)

wholeness during the manipulation of the packaged goods. Thus, a simple approach was adopted to boost the mechanical attributes of the Cu-G-CSN films. The CSN solution was frozen and then the gelling Cu solution was placed over it. The slow diffusion of Cu into the solid frozen CSN would slow the rate of the Cu induced CSN gelation. Slow gelation was formerly shown to create more mechanically stable gels that exhibit more homogeneity [17]. The homogeneity of the newly formed Cu-G-CSN would also elevate its compactness, and this would constitute a barrier against water diffusion and would impede the occurrence of alterations in the Cu-G-CSN films after contacting aqueous solutions which would further promote their exploitation as packaging materials. Noteworthy, this freeze gelation approach was adopted earlier for CSN gelation via NaOH [18], but it was never inspected for Cu induced CSN gelation.

In the current research, Cu-G-CSN films were prepared via freeze-gelation approach. The films were characterized with SEM and UV. Their mechanical and antimicrobial attributes were also inspected as well as their stability in distilled water in order to check their adequacy for application in food packaging.

2. Materials and methods

2.1. Materials

CSN was acquired from Acros Organics, USA. Its molecular weight was stated to be 100-300 kDa. All other chemicals were analar or analogous quality.

2.2. Methods

2.2.1. Fabrication of the Cu-G-CSN films

A 0.8% (v/v) acetic acid solution was exploited to dissolve CSN (3%, w/w). Glycerol was also added to the CSN solution at a 30% (w/w) final concentration. The CSN solution (≈ 8 gm) was then put within plastic petri-dishes (9 cm diameter) and was frozen. Afterwards, the $\text{CuSO}_4 \cdot \text{H}_2\text{O}$ (0.2-2% w/w) gelling solution was placed onto the frozen CSN and was left to interact at room temperature for 3 h. The excess CuSO_4 solution was then discarded, and the formed Cu-G-CSN films were meticulously washed with distilled water and were dried overnight within an oven at 37°C . Finally, the dried Cu-G-CSN films were detached from their mould.

2.2.2. Reckoning of water content

Initially, the surfaces of the wet Cu-G-CSN films, which were washed to eliminate excess CuSO_4 , were gently padded with filter paper in order to accurately weigh them. This weight was their wet weight (W_w). The films dry weight (W_d) was also inspected and it

was their weight after being dried in the oven. Both of these weights were utilized to reckon the water content as follows: $W_w - W_d / W_w * 100$ [2].

2.2.3. Microscopic investigation

Variable dried Cu-G-CSN films had their surfaces and their cross-sections inspected via scan electron microscopy (SEM). This inspection was performed without any additional treatment steps.

2.2.4. Assessment of the Cu-G-CSN films mechanical attributes

The dried Cu-G-CSN films were cut as 1×7 cm² rectangles. Afterwards, these rectangles were pulled within a universal testing machine at a 0.5 mm/sec cross-head speed and with an inceptive grip separation of 3 cm in order to estimate their tensile strength and elongation percent.

2.2.5. Inspection of the films behavior in distilled water

The dried Cu-G-CSN films were cut as 1×3 cm² rectangles. These rectangles were accurately weighed and this weight was the 100%. Afterwards, the rectangles were placed within distilled water and were incubated at 37°C . After 2, 3, & 5 days, these rectangles were picked out of the water, padded with a filter paper, weighed, and returned back to the distilled water at 37°C . The recorded weights were reckoned as percents with respect to the inceptive 100% weights.

2.2.6. UV inspection

The dried Cu-G-CSN films, which were prepared with 0.2-2% (w/w) CuSO_4 , were cut into $1 \text{ cm} \times 3 \text{ cm}$ rectangles. These rectangles were placed in the cuvette holder inside a UV-spectrophotometer and they were scanned within 600-1000 nm wavelength range. Moreover, CuSO_4 and CSN solutions were also individually scanned within the aforementioned range. The acquired spectra were then compared.

2.2.7. Assessment of the Cu-G-CSN films antimicrobial attributes

One centimeter square of the dried Cu-G-CSN films was individually tested against *Candida albicans* NRRL Y-477 and *Staphylococcus aureus* ATCC 29213. Melted serialized potato dextrose agar (for *C. albicans*) or Mueller-Hinton agar (*S. aureus*) were inoculated with the respective organism and were left to cool and solidify. The films were put over the solidified medium. The inoculated plates were then incubated for 24h at 30°C . After incubation time, antimicrobial activity was evaluated

by measuring the zone of inhibition against the test organisms millimeters (mm).

3. Results and discussion

3.1. Effect of the variable CuSO₄ concentrations

3.1.1. Macroscopic features

At all tested CuSO₄ concentrations, firm films were obtained. These films were easily detached from their mould (Figure 1) and they were characterized with their blue see-through appearance. However, the wet weights and water contents of the films diminished progressively upon elevating the CuSO₄ concentrations (Table 1). Moreover, the dry weight of the films dropped significantly (P-value <0.05) from 1.85 gm to 1.40 gm, and then to 1.24 gm upon elevating the CuSO₄ concentration from 0.2 to 0.5 and then 0.7%, respectively. Elevating the CuSO₄ concentration would provide more Cu²⁺ ions to interact with the CSN amino and hydroxyl entities (chelation) [1]. Thus, more co-ordinate bonds would be established within the CSN film. These bonds would help bring the CSN chains nearer to each other. The proximity of the CSN chains would provide more opportunities for the construction of hydrogen-bonds between the CSN functional residues and also between CSN and glycerol (30%). Elevating the CSN films content of co-ordinate and hydrogen bonds would elevate the cross-linking within these films and this would subsequently lessen their free space and cause them to become denser [9]. Lessening the free space of the Cu-G-CSN films could have lessened their dry weight. Moreover, more dense Cu-G-CSN films would present lesser space for water moieties, and this could have triggered the reduction in the wet weight and the water content upon elevating the CuSO₄ concentrations. Similarly, sodium-alginate-CSN films manifested diminution in their water content after elevating the sodium alginate concentration as this elevated the inter-molecular interactions within the films and made them denser [8]

Nevertheless, it was observed that elevating the CuSO₄ concentration beyond 0.7% induced less pronounced reductions in the films wet and dry weights. Actually, the dry weights of the 0.7% and

1% CuSO₄ treated Cu-G-CSN films (Table 1) were statistically insignificant (P-value>0.05) from one another as well as the dry weights of the 1%, 1.5%, and 2% CuSO₄ treated Cu-G-CSN films. Thus, it could be implied that elevating the CuSO₄ concentrations beyond 0.7% didn't largely boost the co-ordinate bonds formation within the Cu-G-CSN films, and hence, the free space and density of the films weren't much reduced, and this led to limited reductions in the films dry and wet weights. This might suggest irregularities in the Cu-CSN interactions at elevated CuSO₄ concentrations. Irregular Cu-CSN interactions were also formerly observed upon elevating the CuSO₄ concentration from 0.2% to 0.5% whilst preparing wet Cu-glutaraldehyde gelled CSN beads. It was argued that such elevation accelerated the CSN gelling rate. This subsequently led to irregular Cu-CSN interactions which were visualized by the deposition of irregular copper aggregates on the surface and within the 0.5% CuSO₄ treated beads [14].

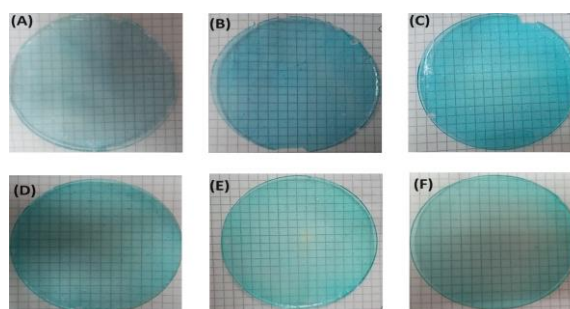


Figure 1: the Cu-G-CSN films acquired via (A) 0.2%, (B) 0.5%, (C) 0.7%, (D) 1%, (E) 1.5%, and (F) 2% CuSO₄ solutions

3.1.2. Microscopic features

It was debated in the previous section that elevating the CuSO₄ concentration beyond 0.7% would disturb the Cu-G-CSN interactions. Thus, the surface and the cross-sections of the 1.5% CuSO₄ treated Cu-G-CSN films (>0.7%) were compared to those of the 0.5% CuSO₄ treated Cu-G-CSN films (<0.7%). The 0.5% CuSO₄ treated Cu-G-CSN films offered a granulated surface (Figures 2A&B).

Table 1: The wet weights, dry weights and water contents of the the Cu-G-CSN films acquired at variable CuSO₄ concentrations

CuSO ₄ concentration (%, w/w)	Wet weight (gm)	Dry weight (gm)	Water content (%)
0.2	17.44±0.19	1.85±0.01	89.58±0.16
0.5	12.57±0.19	1.40±0.02	88.75±0.20
0.7	10.69±0.13	1.24±0.01	88.34±0.13
1	9.61±0.11	1.16±0.02	87.97±0.09
1.5	8.97±0.23	1.07±0.02	87.88±0.33
2	8.53±0.26	1.14±0.03	86.75±0.35

Noteworthy, the dibenzocrown ether cross-linked CSN exhibited a similar surface which was described as bean-like-granulated surface. Such granulation was debated to form secondary to the inter and intra-molecular cross-links within this CSN [19]. Lots of cross-links would also be provided in case of the 0.5% CuSO₄ treated Cu-G-CSN films owing to the bountiful co-ordinate bonds formed amidst CSN and Cu²⁺ and the bountiful hydrogen bonds formed amidst CSN and glycerol and also within CSN. Thus, the granulated surface of the 0.5% CuSO₄ treated Cu-G-CSN films could also be regarded to the bountiful cross-links. It should also be noted that such granulation was only a surface phenomenon as the cross-section of the 0.5% CuSO₄ treated Cu-G-CSN films was compact and pores free (Figures 3A&B). Thus, the films interconnection density wouldn't be lowered and their mechanical attributes wouldn't be reduced. On another occasion, shallow pores were induced on the surface of CSN beads after supplementing their gelling tripolyphosphate solution with 0.2M Na₂CO₃. These shallow pores were also confined to the beads surface and didn't extend into the beads interior. Thus, the beads interconnection density wasn't reduced whereas their available surface area was elevated. This provided more space for the physical and chemical cross-linking and eventually boosted the beads mechanical attributes [20]. Accordingly, it could be implied that the granulation on the 0.5% CuSO₄ treated Cu-G-CSN films would elevate their surface area and provide more space for cross-linking. This would in turn boost their mechanical attributes.

With respect to the 1.5% CuSO₄ treated Cu-G-CSN films, they exhibited smooth surface (Figures 2C&D) and compact pores-free cross-section (Figures 3C&D). Nonetheless, lots of lustrous spots were evident in their cross-section (Figures 3C&D). These lustrous spots were formerly observed in the cross-section of the Cu-glutaraldehyde gelled CSN beads after elevating the CuSO₄ concentration. It was argued that such elevation accelerated the CSN gelling rate. This subsequently led to irregular Cu-CSN interactions which were visualized by the deposition of irregular copper aggregates on the surface and within the Cu-glutaraldehyde gelled CSN beads [14]. The lustrous spots of the 1.5% CuSO₄ treated Cu-G-CSN films confirmed the irregular in the Cu-CSN interactions at concentration beyond 0.7% which led to such irregular copper deposition.

3.1.3. Mechanical attributes

The mechanical attributes of the Cu-G-CSN films, which included their tensile strength (TS) and elongation percent (E%), were studied. The TS refers to the utmost stress a film can endure before its failure; thus, loftier TS values would be needed so

as to maintain the intactness of the packaging. The TS of the Cu-G-CSN films was significantly elevated (P-value<0.05) from 4.74 to 12.84 MPa upon elevating the CuSO₄ concentration from 0.2 to 0.5% (Table 2). It was formerly reported that the cohesion amidst the polymer chains was a determinant for the TS [2]. The cohesion amidst CSN chains would be much improved after elevating the CuSO₄ concentration from 0.2 to 0.5% owing to the increased co-ordinate and hydrogen bonds. Thus, the TS was significantly elevated. Noteworthy, the 12.84 MPa TS recorded for the 0.5% CuSO₄ treated Cu-G-CSN films was finer than the 9.43 MPa TS offered by the CSN/poly(vinylalcohol) electrospun fibrous mats [11]. Furthermore, this TS was amidst the TS range (8.3-31.4 MPa) of the low-density polyethylene, which is a commonly used packaging material [21]. The E% of the 0.5% CuSO₄ treated Cu-G-CSN films (31.86%) was also amidst the E% range (10-1200%) of the low-density polyethylene [21]. Thus, the 0.5% CuSO₄ was considered as the optimal concentration for the Cu-G-CSN films.

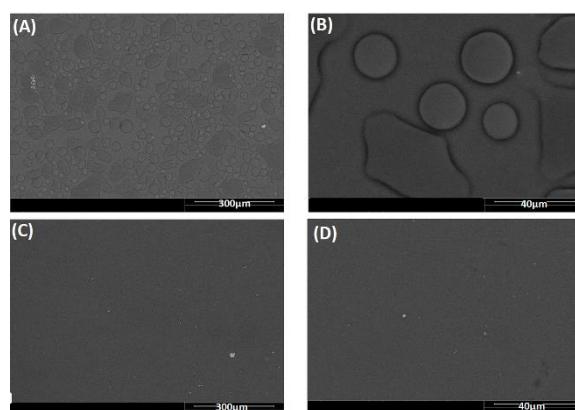


Figure 2: 400X and 3000 X magnification of the surfaces of the 0.5% (A & B) and the 1.5% (C & D) CuSO₄ treated Cu-G-CSN films

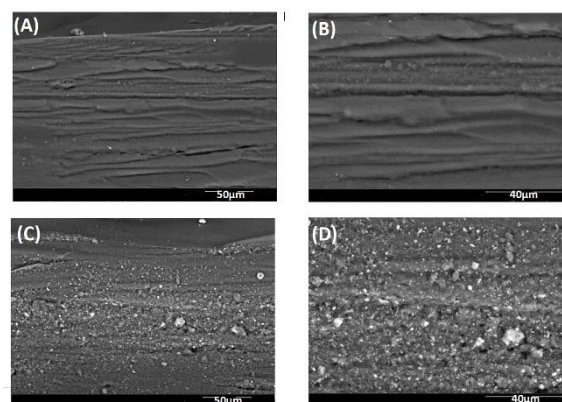


Figure 3: 1500X and 3000 X magnification of the cross-sections of the 0.5% (A & B) and the 1.5% (C & D) CuSO₄ treated Cu-G-CSN films

Table 2 revealed that elevating the CuSO_4 concentration from 0.5% to 0.7% significantly (P -value <0.05) dwindled the TS from 12.84 to 8.26 MPa. The E% of the 0.7% Cu-G-CSN films was also dwindled by -1.92 folds. Further elevating the CuSO_4 concentration from 0.7 to 1.5% induced insignificant (P -value >0.05) fluctuations in the TS. The E% of the films also manifested slight fluctuations amidst 16.21-17.86% along the 0.7-1.5% CuSO_4 concentration range. Noteworthy, in the macroscopic features section, the pattern of the dry weight reductions implied that the irregularities in the Cu-CSN interactions occurred at $> 0.7\%$ CuSO_4 concentration. However, the aforementioned sharp dwindles in the TS and E% of 0.7% treated Cu-G-

CSN films implied that the irregularities in the Cu-CSN interactions occurred earlier at $\geq 0.7\%$ CuSO_4 concentration. Such irregular Cu-CSN interactions were visualized in the 1.5% treated Cu-G-CSN films by the vast irregular deposition of copper aggregates within the films interior (Figures 3C&D). These aggregates would induce discontinuities in Cu-G-CSN films configuration. This in-turn would lessen the films coherence, and thus would lessen its TS [2]. These discontinuities would also lessen the E%. In a similar situation, the discontinuities induced by oil droplets were argued to lessen the TS and E% of the Mung bean starch-guar gum-sunflower seed oil films [22].

Table 2 : The mechanical attributes of the the Cu-G-CSN films acquired at variable CuSO_4 concentrations

CuSO ₄ concentration (%, w/w)	Tensile strength (MPa)	Elongation percent (%)
0.2	4.74±0.32	30.29±1.14
0.5	12.84±0.55	31.86±3.05
0.7	8.26±0.55	16.61±3.75
1	9.44±0.59	17.86±2.08
1.5	8.96±1.02	16.21±5.83

3.1.4. Inspection of the films behavior in distilled water

The weight of the 0.2% CuSO_4 treated Cu-G-CSN films was elevated to 124.22% (Figure 4) following their 48h soaking process (in distilled water at 37°C). However, no significant alterations were recorded when the weight percents, which were recorded for the 0.5-2% CuSO_4 treated Cu-G-CSN films after their 48 h soaking, were compared to their inceptive 100% weights via ANOVA (P -value=0.24118). This implied the elevated stability of the 0.5-2% CuSO_4 treated Cu-G-CSN films. This elevated stability could be regarded to their elevated content of co-ordinate and hydrogen bonds as this would elevate the films cross-linking. Subsequently, the films free space would be lessened and they would become denser [9]. More dense Cu-G-CSN films would present lesser space for water moieties, and thus no significant weight alterations were observed during the 48 h soaking of the 0.5-2% CuSO_4 treated Cu-G-CSN films. Moreover, elevating the films content of co-ordinate and hydrogen bonds would imply that lesser quantities of amino and hydroxyl moieties would be available for the creation of new hydrogen bonds. Thus, fewer spots would be available for hydrogen bonding with water in the cross-linked CSN films [9], and this could have also contributed to the stability of the 0.5-2% CuSO_4 treated Cu-G-CSN films in distilled water (Figure 4).

Noteworthy, the stability the 0.5-2% CuSO_4 treated Cu-G-CSN films was finer than that of the Cu-G-CSN beads, which were formulated after dripping CSN onto CuSO_4 solution. For instance, it was reported that the wet Cu-G-CSN beads swelled in water [13]. Moreover, the dried Cu-G-CSN beads which were formulated via dripping 3% CSN onto 0.06 M CuSO_4 exhibited a swelling ratio of 0.84 following their immersion in simulated ruminal fluid for 24 h [12]. On the other hand the 1% CuSO_4 (=0.056 M $\text{CuSO}_4 \cdot 1\text{H}_2\text{O}$) treated Cu-G-CSN films didn't swell and offered 98.45±0.40% weight after 48 immersion in water. This improved stability could be regarded to the gelation method adopted herein. Placing the CuSO_4 solution onto the frozen CSN would slow diffusion of Cu into the solid frozen CSN. This would slow the rate of the Cu induced CSN gelation. Slow gelation was formerly shown to create more mechanically stable gels that exhibit more homogeneity [17]. The homogeneity of the newly formed Cu-G-CSN would elevate its compactness, and this would constitute a barrier against water diffusion and inhibited the films swelling.

Extending the films soaking time induced weight reductions in all samples (Figure 4). For instance, the 0.5% CuSO_4 treated Cu-G-CSN films kept 91.65±2.04% weight after 7 days. This weight loss could imply slight dissolution in water. Thus, the Cu-G-CSN films wouldn't be preferred for the

packaging of liquid foods, such as milk. They would be more suited for packing solid or semi-solid foods.

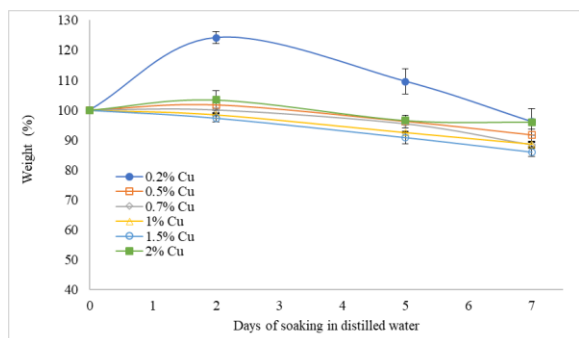


Figure 4 : Weight alterations recorded by the Cu-G-CSN films after soaking them in distilled water at 37°C.

3.1.5. UV inspection

The CuSO_4 solution offered an absorption peak at 807 nm (Figure 5). Similarly, El-Batal et al. [23] observed an absorption peak at 790 nm for CuSO_4 solution. Figure 5 also unveiled that CSN solution didn't offer any characteristic peaks at the inspected 600-1000 nm range whereas peaks were evident in all the Cu-G-CSN films spectra. This confirmed the inclusion of copper within these films. The peak of the 2% CuSO_4 treated Cu-G-CSN films was at 769 nm, which was a little lower than the 807 nm peak of the CuSO_4 solution. Further reducing the CuSO_4 concentration induced further reductions in the locations of the absorption peaks and a 675 nm peak was offered by the 0.2% CuSO_4 treated Cu-G-CSN films.

3.1.6. Inspection of films antimicrobial attributes

All the 0.2-2% CuSO_4 treated Cu-G-CSN films manifested antimicrobial attributes versus both *C. Albicans* and *S. aureus*. Such antimicrobial attributes got more pronounced as the processing CuSO_4 concentration was elevated and this was visualized by the progressive enlargement of the acquired inhibition zones (Table 3). Rather at al. [15] also observed enlargements in the inhibition zones versus *Staphylococcus* after elevating the CuSO_4 concentrations. Moreover, Shiny et al. [16] observed enlargements in the CuSO_4 antimicrobial attributes versus *C. Albicans* after elevating its concentrations. Nonetheless, the antimicrobial attributes manifested by the 0.5% CuSO_4 treated Cu-G-CSN films were still acceptable and this further confirmed the choice of the 0.5% CuSO_4 as the optimal concentration for films preparation.

3.2. Varying the acetic acid concentrations

The concentration of the acetic acid, which was used to solvate CSN, was elevated. Elevating the acetic acid concentration from 0.8% to 1.5% elevated the films wet weights, dry weights and water contents (Table 4). Moreover, further elevating the acetic acid concentration to 2 & 3% inhibited the Cu induced CSN gelation and no films were procured. Elevating the acetic acid concentration would elevate CSN content of protonated amino residues at the expense of the unprotonated amino residues.

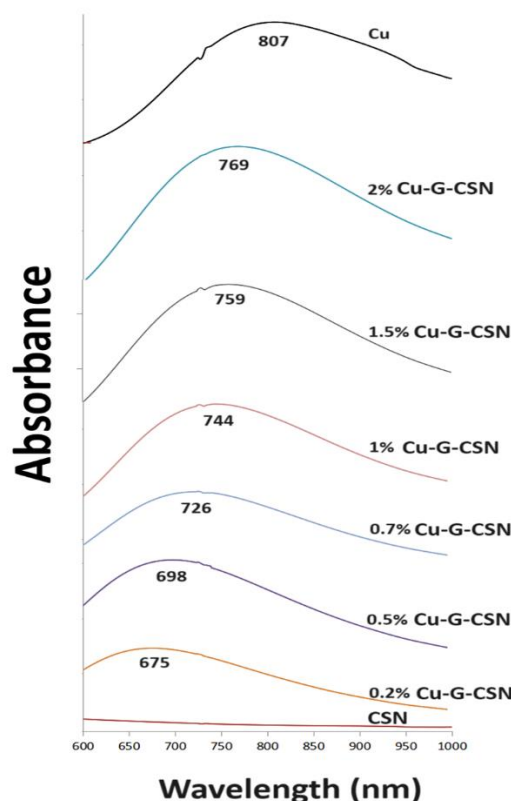


Figure 5: UV spectra of CuSO_4 solution, CSN solution, and the altered Cu-G-CSN films

Table 3: Antimicrobial attributes expressed as inhibition diameter zones in millimeters (mm) of Cu-G-CSN films against the pathological strains based on diffusion assay

CuSO ₄ concentration (% w/w)	Inhibition zones (mm)	
	<i>Candida Albicans</i> NRRL Y-477	<i>Staphylococcus aureus</i> ATCC 29213
0.2	12	11.5
0.5	23.5	20
0.7	25	22
0.8	27.5	25
1	36	34
2	40.5	40

The unprotonated amino residues are the main electron donors which contribute their electron lone pairs to form co-ordinate bonds and chelate metal ions [1]. Thus, reducing CSN content of these unprotonated amino residues would reduce its capability to chelate copper. Hence, the co-ordinate bonds and the cross-linking within the Cu-G-CSN films would be reduced. This would subsequently elevate the films free space and reduce their density. Thus, the films dry weights were elevated. Moreover, more space would be available for water moieties and this would cause the elevation of the films wet weights and water contents. It could also be deduced that when the acetic acid concentration was raised to 2%, the CSN-copper chelation was significantly reduced to the extent that no films were formed. Similarly, Duffy et al. [12] stated that surplus acetic acid was detrimental to the creation of stable Cu-G-CSN beads. Moreover, Kofuji et al. [13] reported that elevating the acetic acid concentration impeded the procurement of spherical Cu-G-CSN beads.

Figure 6 revealed the surface and cross-sections of the 1.5% acetic acid Cu-G-CSN films. The surface was irregular and the cross-sections revealed the in-homogeneity of the films as lots of irregular polymeric lumps were evident. This in-homogeneity was a consequence of the reduced Cu-CSN interactions.

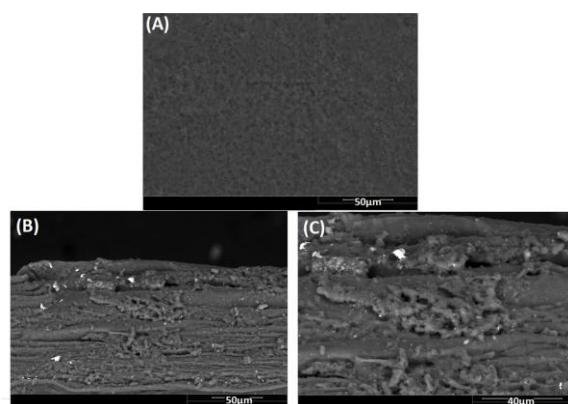


Figure 6: (A) 1500X magnification of the surface of the 0.5% CuSO₄ treated Cu-G-CSN films whose CSN was solvated with 1.5% acetic acid; (B) 1500X and (C) 3000X magnification of the cross-section of these films

4. Conclusions

The 0.5% CuSO₄ treated Cu-G-CSN films which were fabricated via the copper induced freeze-gelling approach were proven to be adequate for packaging applications. Their 12.84 MPa TS and their 31.86% E% were amidst the TS (8.3-31.4 MPa) and E% (10-1200%) ranges of the low-density polyethylene, which is a commonly used packaging material .

Moreover, these films manifested considerable stability in distilled water.

Table 4: The wet weights, dry weights and water contents of the the0.5% CuSO₄ treated Cu-G-CSN films acquired at variable acetic acid concentrations

Acetic acid concentration (% v/v)	Wet weight (gm)	Dry weight (gm)	Water content (%)
0.8	12.57±0.1	1.40±0.0	88.75±0.2
	9	2	0
1	15.08±0.1	1.45±0.0	90.41±0.5
	0	7	1
1.5	16.78±0.2	1.64±0.0	90.20±0.1
2	4	0	3
3		Failed to gel	Failed to gel

5. Conflicts of interest

There are no conflicts to declare.

6. Funding sources

This work was funded by the National Research Centre, Egypt

7. References

- [1]. Mallik A.K., Kabir S.M.F., Rahman F.B.A., Sakib M.N., Efty S.S., Rahman M.M. (2022). Cu(II) removal from wastewater using chitosan-based adsorbents: a review. *J. Environ. Chem. Eng.* 10, 108048.
- [2]. Zhao W. , Liang X. , Wang X. , Wang S. , Wang L., Jiang Y. (2022b). Chitosan based film reinforced with EGCG loaded melanin-like nanocomposite (EGCG@MNPs) for active food packaging. *Carbohydr. Polym.* 290, 119471.
- [3]. Gomaa S.K., Zaki R.A., Wahba M.I., Taleb M.A., El-Refai H.A., El-Fiky A.F., El-Sayed H. (2022). Green method for improving performance attributes of wool fibres using immobilized proteolytic thermozyme. *3Biotech* 12:254.
- [4]. Wahba M.I. (2021) Carrageenan stabilized calcium pectinate beads and their utilization as immobilization matrices. *Biocatal. Agric. Biotechnol.* 35:102078.
- [5]. Wahba M.I. (2022). Gum tragacanth for immobilization of *Bacillus licheniformis* protease: optimization, thermodynamics and application. *React. Funct. Polym.* 179, 105366.
- [6]. Wahba M.I. (2020). Mechanically stable egg white protein based immobilization carrier for β -D-galactosidase: thermodynamics and application in whey lactose hydrolysis. *React. Funct. Polym.* 155:104696.
- [7]. Wahba M.I., Soliman T.N. (2018). Whey protein isolate for the preparation of covalent

- immobilization beads. *Biocatal. Agric. Biotechnol.* 14, 328–337
- [8]. Li X., Shang L., Li D., Wang W., Chen S., Zhong H., Huang Y., Long S. (2022). High-strength, strong-adhesion, and antibacterial polyelectrolyte complex hydrogel films from natural polysaccharides. *Polym. Test.* 109, 107547. <https://doi.org/10.1016/j.polymertesting.2022.107547>.
- [9]. Zhao S., Jia R., Yang J., Dai L., Ji N., Xiong L., Sun Q. (2022a). Development of chitosan/tannic acid/corn starch multifunctional bilayer smart films as pH-responsive actuators and for fruit preservation. *Int. J. Biol. Macromol.* 205, 419–429.
- [10]. Istiqomah A., Utami M.R., Firdaus M., Suryanti V., Kusumaningsih T. (2022). Antibacterial chitosan-Dioscorea alata starch film enriched with essential oils optimally prepared by following response surface methodology. *Food Biosci.* 46:101603.
- [11]. Hosseini S.F., Nahvi Z., Zandi M. (2019). Antioxidant peptide-loaded electrospun chitosan/poly(- vinyl alcohol) nanofibrous mat intended for food biopackaging purposes. *Food Hydrocolloids* 89:637–648.
- [12]. Duffy C., O’Riordan D., O’Sullivan M., Jacquier J.C. (2018). In vitro evaluation of chitosan copper chelate gels as a multimicronutrient feed additive for cattle. *J. Sci. Food Agric.* 98, 4177–4183.
- [13]. Kofuji K., Murata Y., Kawashima S. (2005). Sustained insulin release with biodegradation of chitosan gel beads prepared by copper ions. *Int. J. Pharm.* 303, 95–103.
- [14]. Wahba M.I. (2023). Glutaraldehyde-copper gelled chitosan beads: Characterization and utilization as covalent immobilizers. *Biocatal. Agric. Biotechnol.* 50, 102668.
- [15]. Rather W., Muhee A., Bhat R.A., Haq A.U., Nabi S.U., Malik H.U., Taifa S. (2020). Antimicrobial activity of copper sulphate and zinc sulphate on major mastitis causing bacteria in cattle. *Pharma Innov.* 9:93-95.
- [16]. Shiny E.S., Christian C.B.S.B., Gomathi P. (2023). Screening of Minimal Inhibitory & Fungicidal Concentration of Purified *Thurusa* (Copper Sulphate). *J. Res. Biomed. Sci.* 5, 136-140.
- [17]. Kuo C.K., Ma P.X. (2001). Ionically crosslinked alginate hydrogels as scaffolds for tissue engineering: Part 1. Structure, gelation rate and mechanical properties. *Biomaterials* 22, 511–521. [https://doi.org/10.1016/S0142-9612\(00\)00201-5](https://doi.org/10.1016/S0142-9612(00)00201-5).
- [18]. ElKady A.M., Kamel N.A., Elnashar M.M., Farag M.M. (2021). Production of bioactive glass/chitosan scaffolds by freeze-gelation for optimized vancomycin delivery: Effectiveness of glass presence on controlling the drug release kinetics. *J. Drug Delivery Sci. Technol.* 66:102779.
- [19]. Radwan A.A., Alanazi FK, Alsarra I.A. (2010). Microwave irradiation-assisted synthesis of a novel crown ether crosslinked chitosan as a chelating agent for heavy metal ions (M⁺). *Molecules* 15, 6257-6268.
- [20]. Wahba M.I. (2017). Porous chitosan beads of superior mechanical properties for the covalent immobilization of enzymes. *Int. J. Biol. Macromol.* 105:894–904
- [21]. Othman S.H., Wane B.M., Nordin N., Hasnan N.Z.N., Talib R.A., Karyadi J.N.W. (2021). Physical, mechanical, and water vapor barrier properties of starch/cellulose nanofiber/thymol bionanocomposite films. *Polymers* 13, 4060.
- [22]. Lee J.S., Lee E.s., Han J. (2020). Enhancement of the water-resistance properties of an edible film prepared from mung bean starch via the incorporation of sunflower seed oil. *Sci. Rep.* 10, 13622.
- [23]. El-Batal A.I., El-Sayyad G.S., Mosallam F.M., Fathy R.M. (2020). *Penicillium chrysogenum*-Mediated Mycogenic Synthesis of Copper Oxide Nanoparticles Using Gamma Rays for In Vitro Antimicrobial Activity Against Some Plant Pathogens. *J. Cluster Sci.* 31:79–90.